THE ASTROPHYSICAL JOURNAL, 632:L000–L000, 2005 October 20

MS# 19665 APJL 000(000), pt. 2 Copyeditor: MMG
Monday Oct 03 2005 10:41 AM

DISCOVERY OF X-RAY EMISSION FROM SUPERNOVA 1970G WITH *CHANDRA*: FILLING THE VOID BETWEEN SUPERNOVAE AND SUPERNOVA REMNANTS

STEFAN IMMLER[1,2] AND K. D. KUNTZ[1,3]

Received 2005 June 1; accepted 2005 September 8; published 2005 October XX

ABSTRACT

We report the discovery of X-ray emission from SN 1970G in M101, 35 yr after its outburst, using deep X-ray imaging with the *Chandra X-Ray Observatory*. The *Chandra* ACIS spectrum shows that the emission is soft ($\lesssim$2 keV) and characteristic of the reverse-shock region. The X-ray luminosity, $L_{0.3-2} = (1.1 \pm 0.2) \times 10^{37}$ ergs s^{-1}, is likely caused by the interaction of the supernova shock with dense circumstellar matter. If the material was deposited by the stellar wind from the progenitor, a mass-loss rate of $\dot{M} = (2.6 \pm 0.4) \times 10^{-5}\ M_{\odot}\ \mathrm{yr}^{-1}\ (v_w/10\ \mathrm{km\ s}^{-1})$ is inferred. Utilizing the high-resolution *Chandra* ACIS data of SN 1970G and its environment, we reconstruct the X-ray lightcurve from previous *ROSAT* HRI, PSPC, and *XMM-Newton* EPIC observations, and find a best-fit linear rate of decline of $L \propto t^{-s}$ with index $s = 2.7 \pm 0.9$ over a period of $\approx$20–35 yr after the outburst. As the oldest supernova detected in X-rays, SN 1970G allows, for the first time, direct observation of the transition from a supernova to its supernova remnant phase.

Subject headings: circumstellar matter — supernova remnants — supernovae: individual (SN 1970G) — X-rays: general — X-rays: individual (SN 1970G, M101)

1. INTRODUCTION

Since the launch of the *Chandra* and *XMM-Newton* observatories, the number of supernovae (SNe) detected in X-rays in their near aftermath has more than doubled (see Immler & Lewin [2003] for a review).[4] The high-quality X-ray spectra have confirmed the validity of the circumstellar interaction models (see Fransson et al. 1996, and references therein), which predict a hard spectral component ($\gtrsim$10 keV) for the forward-shock emission during the early epoch ($\lesssim$100 days) and a soft thermal component ($\lesssim$1 keV) for the reverse-shock emission after the expanding shell has become optically thin. The soft emission component dominates the X-ray output of the interaction regions due to its higher emission measure and higher electron densities. This expected "softening" of the X-ray spectrum has been observationally confirmed for a number of young SNe, such as SNe 1978K (Schlegel et al. 2004), 1979C (Immler et al. 2005), 1993J (Zimmermann & Aschenbach 2003), 1999em, and 1998S (Pooley et al. 2002).

Where sufficient data are available, X-ray light curves could be established over significant timescales (e.g., $\approx$25 yr for SNe 1978K and 1979C; Schlegel et al. 2004, Immler et al. 2005; $\approx$8 yr for 1993J; Immler et al. 2001, Zimmermann & Aschenbach 2003). However, little is known about the transition from a young SN into its supernova remnant (SNR) phase, as there have been only a few detections of intermediate-age (25–300 yr) SNe in the radio and none in X-rays. While the X-ray emission of SNe is dominated by the interaction of the shock with the ambient circumstellar matter (CSM), likely deposited by the progenitor's stellar wind, the emission from a SNR is thought to originate in the shocked interstellar medium (ISM). At an age of $\approx$35 yr, SN 1970G is the oldest SN detected in X-rays and closes this gap, allowing one, for the first time, to witness the transition from a SN to its SNR phase.

As the first SN detected in the radio band (Gottesman et al. 1972), just 1 month after its peak optical brightness (1970 July 30; Detre 1970), SN 1970G held the key to our understanding of SN events and the interaction of a SN shock with its environment. Twenty years after the explosion, SN 1970G was rediscovered at 3.5 cm and 20 cm at flux densities similar to other radio SNe, such as SNe 1950B, 1957D, 1961V and 1968D at the same epochs in their evolution, but showed a remarkably fast rate of decline, with a power-law index of -1.95 ± 0.17 (Cowan et al. 1991). Subsequent radio monitoring confirmed this fast rate of decline, followed by a flattening of the radio light curve at an epoch of $\approx$30 yr, which was discussed in the context of the SN shock running into the denser ISM, indicating the onset of the SNR phase (Stockdale et al. 2001).

In this paper we report on the *Chandra* X-ray observation of SN 1970G, as well as previous X-ray data from *ROSAT* and *XMM-Newton*. In § 2 we briefly describe the data and analysis thereof and report on the X-ray spectrum and multimission X-ray light curve in § 3. We discuss the results in the context of the CSM interaction model and put SN 1970G in the context of the evolution from a SN to a SNR in § 4, followed by a summary in § 5.

2. DATA PROCESSING AND ANALYSIS

SN 1970G has been observed with the *Chandra X-Ray Observatory* as part of the 1 Ms observation of the host galaxy M101 (NGC 5457; K. D. Kuntz 2005, in preparation). Five individual *Chandra* ACIS observations (sequence numbers 600389, 600389, 600389, 600389, 600389) from 2004 July 5–11 were merged into a single observation, resulting in a cleaned and exposure-corrected on-source exposure time of 139.5 ks for the ACIS-S2 chip. Details of the data calibration and analysis will be explained in K. D. Kuntz (2005, in preparation). The high-resolution ($\approx$0.″5 FWHM) *Chandra* data were used to search for X-ray emission from the position of SN 1970G, and to examine the contamination by nearby X-ray sources. A *Chandra* ACIS-S2 image of SN 1970G and its environment is given in Figure 1.

We further constructed the long-term X-ray light curve of SN 1970G by extracting source counts from previous *ROSAT*

[1] Exploration of the Universe Division, X-Ray Astrophysics Laboratory, Code 662, NASA Goddard Space Flight Center, Greenbelt, MD 20771.
[2] Universities Space Research Association, Columbia, MD 21044.
[3] Henry A. Rowland Department of Physics and Astronomy, The Johns Hopkins University, 3400 Charles Street, Baltimore, MD 21218.
[4] A complete list of X-ray SNe and references is available at http://lheawww.gsfc.nasa.gov/users/immler/supernovae_list.html.

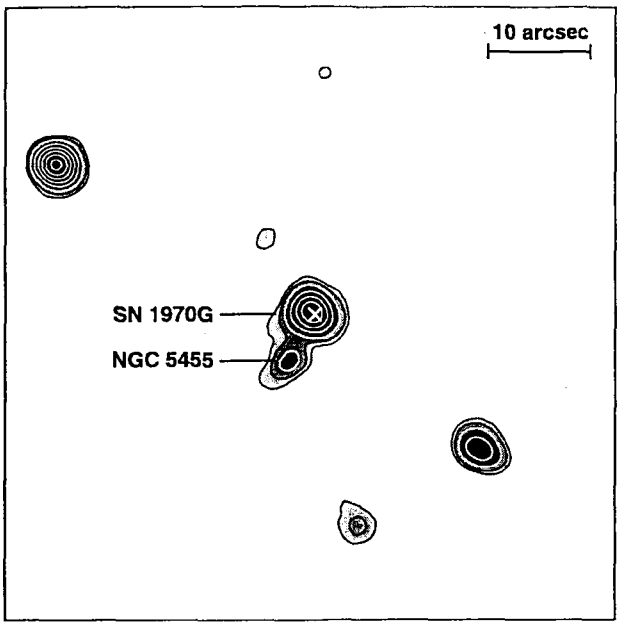

FIG. 1.—Full-band (0.3–8 keV) *Chandra* ACIS-S2 image of the region (size 1 × 1) around the position of SN 1970G. The image is smoothed with a Gaussian of 2.″5 (FWHM) and is given in logarithmic gray scale ranging from 0–1.5 counts pixel^{-1} (1 pixel corresponds to 0.″5). Contour lines are 0.2, 0.4 (*black*), 0.6, 0.8, 1, 1.2, 1.4, and 1.6 counts pixel^{-1} (*white*). The radio position of SN 1970G (Cowan et al. 1991) northeast of the H II region NGC 5455 is marked by a white cross.

HRI (sequence numbers RH600820N00, RH600820A01; merged exposure time 176.1 ks) and *ROSAT* PSPC observations (sequence number RP600108N00; exposure 34.5 ks). Archival *XMM-Newton* EPIC observations (ObsID 0104260101, 43.3 ks; 0164560701, 41.8 ks; 0212480201, 32.4 ks) were also analyzed according to standard analysis procedures described in the *XMM-Newton* ABC Guide, version 2.01.[5]

A short (2.8 ks) *Einstein* HRI observation 154 days after the outburst of SN 1970G did not result in the detection of the SN and is not included in this study. Archival *ASCA* observations were not used due to the large aperture (≈1′ FWHM) and contamination by nearby X-ray sources. The *ROSAT* and *XMM-Newton* count rates were further compared to the published results by Wang et al. (1999; *ROSAT*) and Jenkins et al. (2005; *XMM-Newton*).

3. RESULTS

A pointlike X-ray source is detected at the radio position of SN 1970G (Cowan et al. 1991), with an offset (≲0.″5) similar to the spatial resolution and astrometry of the *Chandra* observation (see Fig. 1). SN 1970G is spatially resolved and well separated from a nearby (≈5″) H II region NGC 5455. Extracting exposure-, background-, and aperture-corrected counts from the position of SN 1970G gives a count rate of (4.3 ± 0.6) × 10^{-4} counts s^{-1}. While the limited photon statistics do not allow a detailed characterization of the energy distribution of the recorded photons, spectral analysis shows that the emission is soft, with the bulk of the emission being confined to the ≲2 keV band.

Adopting a kT = 0.6 keV thermal plasma spectrum typical for the late-time (≳100 days) emission of SNe and assuming a Galactic foreground column density with no intrinsic absorption (N_H = 1.16 × 10^{20} cm^{-2}; Dickey & Lockman 1990) gives a 0.3–2 keV flux and luminosity of $f_{0.3-2}$ = (1.8 ± 0.3) × 10^{-15} ergs cm^{-2} s^{-1} and $L_{0.3-2}$ = (1.1 ± 0.2) × 10^{37} ergs s^{-1}, respectively, for a distance of 7.2 Mpc (Stetson et al. 1998).

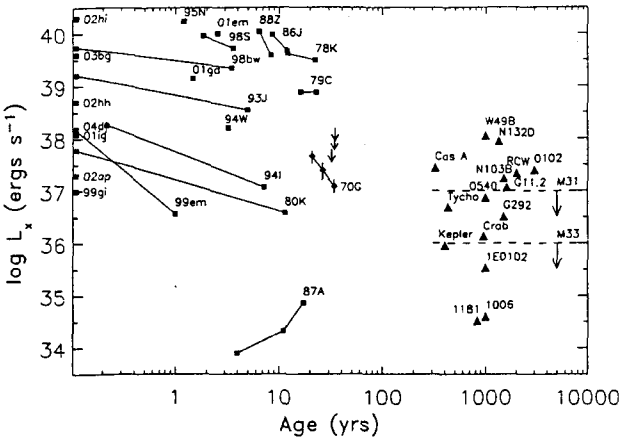

FIG. 2.—Soft-band (0.3–2 keV) X-ray luminosities of all SNe detected to date (*filled squares*) and historical SNRs (*filled triangles*) as a function of age (in units of years). The X-ray light curve of SN 1970G is marked by filled diamonds with error bars (*left to right*: *ROSAT* PSPC, *ROSAT* HRI and *Chandra* ACIS). *XMM-Newton* EPIC upper limits are indicated by arrows.

Since no information is available about the spectral evolution of SN 1970G or other SNe at this age, we used the same spectral template to convert *ROSAT* and *XMM-Newton* count rates into fluxes and luminosities to construct the long-term (≈20–35 yr) X-ray light curve.

An X-ray source is visible in the *ROSAT* HRI images of M101 at the position of SN 1970G (see Fig. 2 in Wang et al. 1999). The source, however, is not included in the *ROSAT* HRI catalog since it is slightly below the employed detection threshold (S/N = 3.5; Wang et al. 1999). Extraction of source counts within the HRI aperture and subtraction of emission from the nearby H II region NGC 5455 ($L_{0.3-2}$ = 2.2 × 10^{36} ergs s^{-1}) gives a luminosity of $L_{0.3-2}$ = (2.6 ± 0.6) × 10^{37} ergs s^{-1}.

An X-ray source is also listed in the *ROSAT* PSPC catalog at the position of SN 1970G (source P12; Wang et al. 1999), with a signal-to-noise ratio of S/N = 4.5. We used the high-resolution *Chandra* observation and subtracted the integrated flux of all detected *Chandra* sources from the *ROSAT* PSPC flux within the PSPC aperture (≈25″ FWHM). Assuming that the residual emission arises from the SN itself, we obtain a luminosity of $L_{0.3-2}$ = (4.9 ± 1.1) × 10^{37} ergs s^{-1}.

A faint X-ray source is visible in each of the nine *XMM-Newton* pn, MOS1, and MOS2 images at low energies (<2 keV). No photons were recorded in the hard (2–6 keV) band. The source, however, is extended (≈20″) and shows no concentration of the recorded photons at the radio position of SN 1970G. Since it is likely that the emission is contaminated by the nearby H II region and other soft emission components inside the Galactic disk due to the larger aperture of the EPIC instruments (≈6″ FWHM), we only use the inferred count rates as upper limits. Discrepancies between the published pn and MOS count rates for source 44 (factor of 16.5; Jenkins et al. 2005), corresponding to SN 1970G, for one of the published *XMM-Newton* data (ObsID 0104260101) make a comparison problematic.

We calculated the mass-loss rate of the progenitor as a function of the stellar wind age using the relationship L_x =

[5] Available from http://heasarc.gsfc.nasa.gov/docs/xmm/abc/.

TABLE 1
X-RAY PROPERTIES OF SN 1970G

Epoch (yr)	Date	Instrument	Count Rate (10^{-4} counts s^{-1})	$f_{0.3-2}$ (10^{-15} ergs cm^{-2} s^{-1})	$L_{0.3-2}$ (10^{-37} ergs s^{-1})	$\dot{M}$ (10^{-5} $M_\odot$ yr^{-1})
20.9	1991 Jun 8–9	*ROSAT* PSPC	9.0 ± 2.1	7.9 ± 1.8	4.9 ± 1.1	3.2 ± 0.7
26.1	1996 May 14–Nov 23	*ROSAT* HRI	1.8 ± 0.4	4.2 ± 0.9	2.6 ± 0.6	2.7 ± 0.6
31.9	2002 Jun 4	*XMM-Newton* EPIC	<48.3	<10.2	<6.3	<5.8
34.0	2004 Jul 5–11	*Chandra* ACIS	4.3 ± 0.6	1.8 ± 0.3	1.1 ± 0.2	2.6 ± 0.4
34.0	2004 Jul 23	*XMM-Newton* EPIC	<80.6	<17.0	<10.6	<7.7
34.5	2005 Jan 8	*XMM-Newton* EPIC	<119.3	<25.2	<15.6	<9.4

$4/(\pi m^2)\Lambda(T) \times (\dot{M}/v_w)^2 \times (v_s t)^{-1}$, where m is the mean mass per particle (2.1×10^{-27} kg for a H+He plasma), $\Lambda(T)$ the cooling function of the heated plasma at temperature T, $\dot{M}$ the mass-loss rate of the progenitor, v_w the speed of the stellar wind blown off by the progenitor, and v_s the speed of the outgoing shock (see Immler et al. 2002). A constant shock velocity of $v_s = 9000$ km s^{-1}, similar to other core-collapse SNe, such as SN 1979C (Marcaide et al. 2002) was assumed. An effective (0.3–2 keV band) cooling function of $\Lambda = 3 \times 10^{-23}$ ergs cm^{-3} s^{-1} for an optically thin thermal plasma with a temperature of 10^7 K was adopted, which corresponds to the assumed thermal plasma temperature. Assuming different plasma temperatures in the range 0.5–1 keV would lead to changes in the emission measure of $\lesssim$10%. Key observational properties of SN 1970G are listed in Table 1.

4. DISCUSSION

Previous X-ray observations of SN 1970G with *ROSAT*, *ASCA*, and *XMM-Newton* lacked the spatial resolution needed to separate the SN from the nearby (≈5″) H II region NGC 5455. Using the subarcsecond *Chandra* imaging capability, in combination with the deep exposure time (140 ks), we detect soft ($\lesssim$2 keV) X-ray emission from SN 1970G with a luminosity of $L_{0.3-2} \approx 1 \times 10^{37}$ ergs s^{-1}, 35 yr after its outburst. The source is spatially resolved from the nearby H II region NGC 5455 (≈5″), which is observed at a $\lesssim$20% flux level compared to SN 1970G.

Given the spatial information from the high-resolution *Chandra* imaging, we recover X-rays from SN 1970G in the *ROSAT* HRI and PSPC observations. SN 1970G is not conclusively detected in three recent (2002–2005) *XMM-Newton* observations due to the extent of the source (≈20″) as imaged by the pn and MOS instruments, and positional offsets larger than the instrumental uncertainties (≈5″).

In combination, the multimission X-ray data show a constant rate of decline which confirms that the emission is due to the SN itself. The rate of decline of $L \propto t^{-s}$ with index $s = 2.7 \pm 0.9$ is rather steep and similar to the X-ray rates of decline observed for the Type IIn SNe 1986J ($L_X \propto t^{-3}$; Temple et al. 2005) and 1988Z ($t^{-3.9}$; Aretxaga et al. 1999). Since we cannot conclusively exclude additional contamination of the earlier *ROSAT* data with unresolved X-ray emission components in M101, our inferred rate of decline is rather conservative.

The rate of decline inferred from the X-ray data is consistent with the slope of the radio decay (-1.95 ± 0.17; Stockdale et al. 1991), which confirms that the emission probes similar regions in the shocked CSM. The X-ray data, however, do not show the flattening of the decay at an age of ≈30 yr, as seen in the 20 cm radio data (-0.29 ± 0.13). While this might be due to the limited number of X-ray data points, it could also indicate that the reverse shock, which produces the X-rays and travels at a speed of some 1000 km s^{-1} slower than the forward shock, has not yet reached the dense ISM, which is probed by the radio emission originating in the forward shock.

The lack of X-rays above 2 keV confirms that the emission is soft and likely thermal. Such a soft spectrum is expected for the late emission of a SN, where the shocked plasma emission is the product of the reverse shock interaction.

Assuming that the emission arises from shock heated plasma deposited by the progenitor's stellar wind, a mass-loss rate of $\dot{M} = (2.6 \pm 0.4) \times 10^{-5}$ $M_\odot$ yr^{-1} $(v_w/10$ km $s^{-1})$ is inferred for the late epoch observed with *Chandra*. The mass-loss rates inferred from the *ROSAT* PSPC and HRI data [(3.2 ± 0.7) and $(2.7 \pm 0.6) \times 10^{-5}$ $M_\odot$ yr^{-1} $(v_w/10$ km $s^{-1})$] are consistent with a constant mass-loss rate over a period of ≈20–35 yr after the peak optical brightness. This corresponds to ≈19,000–31,000 yr in the stellar wind age, using the conversion $t_w = tv_s/v_w$ and assuming a stellar wind speed of 10 km s^{-1} and a shock front velocity of 9000 km s^{-1}.

Our inferred mass-loss rate is consistent with that derived from radio monitoring [2×10^{-5} $M_\odot$ yr^{-1} $(v_w/10$ km $s^{-1})$; Weiler 1993]. Furthermore, the measured mass-loss rate for SN 1970G is similar to those inferred for other young ($\lesssim$20 yr) Type II SNe, which typically range from 10^{-5} to 10^{-4} $M_\odot$ yr^{-1} (see Immler & Lewin 2003). This indicates that the X-ray emission arises from shock-heated CSM deposited by the progenitor rather than shock-heated ISM, even at this late epoch after the outburst.

In the absence of a dense ISM, the X-ray evolution of a core-collapse SN into a SNR can be described by a simple power law. X-ray luminous SNe, such as SN 1993J, can therefore evolve into X-ray–luminous SNRs such as Cas A ($L_{0.3-2} = 2.8 \times 10^{37}$ ergs s^{-1} at an age of ≈320 yr) with a swept-up gas mass around 4 $M_\odot$ (Dunne et al. 2003) if the measured mass-loss rate of $\approx 10^{-4}$ $M_\odot$ yr^{-1} is sustained over a period of some 10^4 yr.

In Figure 2 we plot the X-ray evolution of all SNe detected to date,[6] as well as the X-ray luminosities of historical SNRs in the Galaxy, LMC, SMC (as observed with *Chandra*[7]), M31 (Supper et al. 2001; Kong et al. 2003), and M33 (Ghavamian et al. 2005). A comparison of the X-ray luminosities of the core-collapse SNe (visible in the left part of Fig. 2) with well-evolved SNRs (right part of Fig. 2) shows that the transition from a SN to a SNR appears to be rather smooth (see also Fig. 2 in Stockdale et al. 2001). If the evolution of SN 1970G continues as observed to date, it will be similar to X-ray–faint Galactic SNRs such as SNRs 1181 and 1006 ($L_X \approx 10^{34}$ ergs s^{-1}). If the light curve flattens significantly after encountering a dense ISM (as in the case of SNRs as a result from Type Ia SNe such as Tycho), SN 1970G might evolve into a more luminous SNR such as Kepler or the Crab ($\approx 10^{36}$ ergs s^{-1}). The observed flattening of the radio

[6] See http://lheawww.gsfc.nasa.gov/users/immler/supernovae_list.html.
[7] See http://www.astro.psu.edu/users/green/Main/main5.html.

q7 light curve with a power-law slope change from -1.95 ± 0.17 to -0.29 ± 0.13 at an age of $\approx$30 yr (Stockdale et al. 1991) might indicate such as scenario.

X-ray–bright SNe such as SNe 1978K (Schlegel et al. 2004) and 1979C (Immler et al. 2005), which show no signs of an X-ray decline out to large distances ($\gtrsim 10^{17}$ cm) from the sites of the explosion, can evolve into luminous SNRs such as Cas A through their strong interactions with dense stellar winds alone. In case the shock encounters a dense ISM at a later stage, these SNe have the potential to attain even higher X-ray luminosities as observed for the brightest SNRs (such as W49B q8 or N132D).

Clearly, long-term monitoring of known X-ray SNe and new detections of intermediate-age (around 100 yr) SNe in X-rays are needed to address these questions and to study the transition from a SN into a SNR in more detail. Deep galaxy surveys with *Chandra* and *XMM-Newton* and future X-ray missions such as *Constellation-X* and *XEUS* will provide the capabilities to detect these intermediate-age SNe in the near future and to fill the void in the evolution of a SN to a SNR.

5. SUMMARY

Key results based on our deep (140 ks) X-ray observation of SN 1970G in M101 are:

1. SN 1970G is detected with a luminosity of $L_{0.3-2} = (1.1 \pm 0.2) \times 10^{38}$ ergs s^{-1}, 35 yr after its outburst in our deep *Chandra* observation of M101.
2. SN 1970G is recovered in previous *ROSAT* HRI and PSPC observations and shows a best-fit linear rate of decline of $L \propto t^{-s}$ with index $s = 2.7 \pm 0.9$ over the observed period of 20–35 yr after its outburst, consistent with the observed radio decay for an epoch $\lesssim$30 yr.
3. The emission of SN 1970G is soft ($\lesssim$2 keV) and indicates that it originates in the reverse-shocked region, as expected for the late emission in the evolution of a SN.
4. A mass-loss rate of $\dot{M} = (2.6 \pm 0.4) \times 10^{-5}\ M_{\odot}\ \mathrm{yr}^{-1}$ is inferred consistent with being constant over a period of 19,000–31,000 yr in the evolution of the progenitor.
5. At an age of 35 yr, the SN shock has not yet encountered a denser ISM, which would mark the start of the SNR phase and is likely to occur at a later stage in the evolution ($\approx$50–100 yr).
6. Comparison of the X-ray light curves of all SNe detected to date with the X-ray luminosities of SNRs indicates a smooth transition of SNe into their SNR phases.

The authors wish to thank R. Petre and the anonymous referee for helpful suggestions. K. D. K. was supported by the *Chandra* grant SAO GO-5600587.

REFERENCES

Aretxaga, I., et al. 1999, MNRAS, 309, 343
Cowan, J. J., Goss, W. M., & Sramek, R. A. 1991, ApJ, 379, L49
q9 Detre, L. 1970, IAU Circ. 2269
Dickey, J. M., & Lockman, F. J. 1990, ARA&A, 28, 215
Dunne, L., Eales, S., Ivison, R., Morgan, H., & Edmunds, M. 2003, Nature, 424, 285
Fransson, C., Lundqvist, P., & Chevalier, R. A. 1996, ApJ, 461, 993
Ghavamian, P., Blair, W. P., Long, K. S., Sasaki, M., Gaetz, T. J., & Plucinsky,
q10 P. P. 2005, AJ, 130, 539
Gottesman, S. T., Broderick, J. J., Brown, Robert L., Balick, B., & Palmer, P. 1972, ApJ, 174, 383
Houck, J. C., Bregman, J. N., Chevalier, R. A., & Tomisaka, K. 1998, ApJ,
q11 493, 431
Immler, S., Aschenbach, B., & Wang, Q. D. 2001, ApJ, 561, L107
Immler, S., & Lewin, W. 2003, in Supernovae and Gamma-Ray Bursters, ed. K. Weiler (Berlin: Springer), 91
Immler, S., Wilson, A. S., & Terashima, Y. 2002, ApJ, 573, L27
Immler, S., et al. 2005, ApJ, 632, 283
Jenkins, L. P., Roberts, T. P., Warwick, R. S., Kilgard, R. E., & Ward, M. J. 2005, MNRAS, 357, 401
Kong, A. K. H., DiStefano, R., Garcia, M. R., & Greiner, J. 2003, ApJ, 585, 298
Marcaide, J. M., et al. 2002, A&A, 384, 408
Pooley D., et al. 2002, ApJ, 572, 932
Schlegel, E. M., Kong, A., Kaaret, P., DiStefano, R., & Murray, S. 2004, ApJ, 603, 644
Stetson, P. B., et al. 1998, ApJ, 508, 491
Stockdale, C. J., Goss, W. M., Cowan, J. J., & Sramek, R. A. 2001, ApJ, 559, L139 q12
Supper, R., Hasinger, G., Lewin, W. H. G 2001, A&A, 373, 63
Temple, R., Raychaudhury, S., & Stevens, I. 2005, MNRAS, in press (astro-ph/0506657) q13
Wang, Q. D., Immler, S., & Pietsch, W. 1999, ApJ, 523, 121
Weiler, K. W. 1993, in ASP Conf. Ser. 35, Massive Stars: Their Lives in the Interstellar Medium, ed. J. P. Cassinelli & E. B. Churchwell (San Francisco: ASP), 436
Zimmermann, H.-U., & Aschenbach, B. 2003, A&A, 406, 969